

Changing Relationships Between Sunspot Number, Total Sunspot Area and $F_{10.7}$ in Cycles 23 and 24

Ken Tapping¹  · Carly Morgan² 

Received: 21 February 2017 / Accepted: 9 May 2017 / Published online: 23 May 2017
© Springer Science+Business Media Dordrecht 2017

Abstract This article is an update of a study (Tapping and Valdès in *Solar Phys.* **272**, 337, 2011) made in the early part of Cycle 24 using an intercomparison of various solar activity indices (including sunspot number and the 10.7 cm solar radio flux), in which it was concluded that a change in the relationship between photospheric and chromospheric/coronal activity took place just after the maximum of Cycle 23 and continued into Cycle 24. Precursors (short-term variations) were detected in Cycles 21 and 22. Since then the sunspot number index data have been substantially revised. This study is intended to be an update of the earlier study and to assess the impact of the revision of the sunspot number data upon those conclusions. This study compares original and revised sunspot number, total sunspot area, and 10.7 cm solar radio flux. The conclusion is that the transient changes in Cycles 21 and 22, and the more substantial change in Cycle 23, remain evident. Cycle 24 shows indications that the deviation was probably another short-term one.

Keywords Solar Activity Cycle · Sunspot number · Total sunspot area · 10.7 cm solar radio flux

1. Introduction

The Sun may be in the process of a significant behavioural change. The minimum between Cycles 23 and 24 was unusually long, and the maximum of Cycle 24 (now past) was the lowest since Cycle 14. Penn and Livingston (2006, 2011) reported umbral magnetic field strengths in sunspots declining by about 50 G per year since the late 1990s. Janardhan, Bisoi, and Gosain (2010) reported a steady decline in the strength of photospheric magnetic

✉ K. Tapping
Ken.Tapping@nrc-cnrc.gc.ca

✉ C. Morgan
Cmmorgan@uvic.ca

¹ National Research Council, PO Box 248, Penticton, British Columbia, V2A 6J9, Canada

² University of Victoria, 3800 Finnerty Rd, Victoria, BC V8P 5C2, Canada

fields at latitudes higher than about 45 degrees since 1990. Tapping and Valdés (2011) compared the 10.7 cm solar radio flux ($F_{10.7}$) with sunspot number and various other indices of photospheric and coronal activity and concluded that in the latter part of Cycle 23 there appeared a significant excess of $F_{10.7}$ over what would have been expected on the basis of sunspot number values, and that this marked a change in the relationship between photospheric and chromospheric/coronal activity. Livingston, Penn, and Svalgaard (2012) made a similar comparison and reached the same conclusion but described it inversely, as a decline in sunspot number compared with what would have been expected on the basis of $F_{10.7}$ values, with the deviation starting around 1995. However, Tapping and Valdés (2011) reported transient changes in Cycles 21 and 22, where around the cycle maxima, there were excesses of $F_{10.7}$ over sunspot number that disappeared during the decline of the cycles. In Cycle 23 the deviation became ongoing, with the deviation increasing steadily, as reported by Livingston, Penn, and Svalgaard (2012). This and other pieces of evidence that solar behaviour is changing were discussed by Janardhan *et al.* (2015). We are now in the declining phase of Cycle 24 and an updated study is timely.

Current solar behaviour may herald a more significant change: short term or longer term. The Sun has exhibited significant changes in behaviour before, where for several solar activity cycles some indices of solar activity fell to very low levels, after which activity returned to “normal” (Eddy, 1976a,b, 1977, 1979). The most dramatic of these in recent history were the Maunder (1645–1714) (Eddy, 1976a) and Dalton (1790–1830) (Komitov and Kafan, 2004) Minima. These might be special events or part of a continuum of behavioural changes.

The various solar activity indices reflect the impact of the solar magnetic activity cycle on different places and sets of processes in the Sun. Intercomparison can therefore show differences in how solar activity manifests itself in different parts of the Sun, providing an additional, more sensitive means to detect changes. It also provides a means to reduce instrumental and other non-solar effects embedded in the data. Ultimately, variations in solar activity indices are driven by the solar activity cycle, which itself is driven by the solar dynamo(s) (Choudhuri, 2003; Athay and Warwick, 1961; Lockwood and Stamper, 1999). Simulations of the solar activity cycle based upon the classical Babcock–Leighton model by Charbonneau, Blais-Laurier, and St-Jean (2004) and Charbonneau, St-Jean, and Zacharias (2005) show, along with the solar activity cycles, behavioural changes ranging from small ones to extended periods of low activity resembling the Maunder and Dalton Minima.

The sunspot number index is non-physical, and therefore not easily amenable to absolute calibration. This makes it harder to avoid long-term calibration drift, particularly since the data were obtained by a long succession of observers and instruments. However, despite these issues, the data have been integrated into one of the most useful records of solar activity, extending back at least 300 years. A sunspot number database maintained by the Royal Observatory, Belgium has just been reviewed, better integrated and recalibrated (Clette *et al.*, 2016; Clette and Lefèvre, 2016). The 10.7 cm solar radio flux is an absolutely measured physical solar quantity, but dates back only to 1947. This index is discussed in detail by Tapping (2013).

In this study we compare i) $F_{10.7}$ with the sunspot number index, ii) $F_{10.7}$ with total sunspot area, and iii) total sunspot area with sunspot number. In each case the comparisons with sunspot number are done for both the original and revised data. We also compare the two sunspot number time-series.

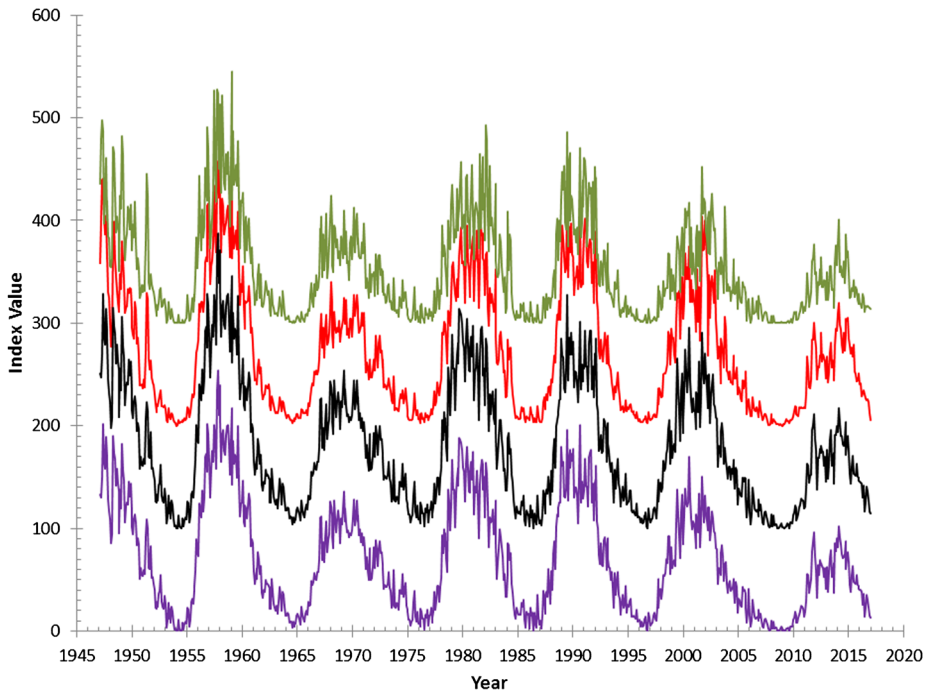


Figure 1 Starting from the bottom, scaled and offset plots of original sunspot number (purple), revised sunspot number (black), 10.7 cm solar radio flux (red), and total sunspot area (green).

2. The Data

The study uses three activity indices: sunspot number, total sunspot area, and the 10.7 cm solar radio flux. These particular indices are selected because of the length of their time-series. The indices and their sources are listed below.

The index data used in the study are shown in Figure 1. The data are monthly averages, additionally smoothed with a 10-month running mean (the reasons for this are given in Section 3). They have been offset and scaled to fit onto a common plot. The original and revised values of the sunspot number index are plotted separately.

2.1. Sunspot Number

The sunspot number record is by far the longest series of direct indications of solar magnetic activity available, dating back at least 300 years. It is a count of visible sunspots, and includes procedures for estimating the numbers of spots in groups, *etc.* Standardised procedures are applied to incorporate data from many observers, instruments and facilities. The data used here are provided by the Solar Influences Data Centre, which is part of the Royal Observatory, Belgium (<http://www.sidc.be/silso/datafiles>). The original sunspot number data have been extensively revised and recalibrated. The data and the recalibration procedures were discussed in Clette *et al.* (2016) and Clette and Lefèvre (2016). The provision of these data (in a form consistent with the revised data set) is continuing. For comparison purposes we use both the original and revised sunspot data, and include an intercomparison of the two.

2.2. Total Sunspot Area

Observations of the total area of all sunspots visible on the solar disc form a consistent data set dating back to 1874. They were originally recorded at the Royal Greenwich Observatory (UK). In 1976 the observations were taken over by the US Air Force, with help from the US National Oceanic and Atmospheric Administration (NOAA). Funding for this programme ended in 2005. The providers of the data have indicated they will keep providing these valuable data as long as possible, but the future of these observations is uncertain. There is comprehensive information about this quantity on the measurements website from which we obtained the data (<http://solarscience.msfc.nasa.gov/greenwch.shtml>). See also Sarychev and Roshchina (2006).

2.3. The 10.7 cm Solar Radio Flux ($F_{10.7}$)

The 10.7 cm solar radio flux is the integrated emission at 10.7 cm wavelength from the solar disc and all sources on it. The emission originates in the upper chromosphere and lower corona, and is a widely used index of solar magnetic activity. It comprises mainly contributions from two emission processes: gyroresonance from thermal plasmas trapped in the intense magnetic fields overlying sunspots, and bremsstrahlung from thermal plasmas overlying the main body of the active region. There may also be an occasional contribution of non-thermal emission, mainly due to the gyrosynchrotron mechanism. These and other solar processes were discussed in detail by Kundu (1965) and Krüger (1979). The $F_{10.7}$ time-series dates back to 1947. It is described in Tapping (2013). The data used here are produced by the National Research Council of Canada and can be obtained from <http://www.spaceweather.gc.ca>.

$F_{10.7}$ shares with the sunspot number index its wide use as a standard indicator of the level of solar magnetic activity. Comparison with the solar magnetic field (e.g. <http://hmi.stanford.edu/hminuggets/?p=1510>) shows that $F_{10.7}$ is an excellent proxy for the disc-average magnetic field. There is a well-known relation between solar EUV and $F_{10.7}$.

All long-term monitoring programmes inevitably involve changes that may impact particular points in the time-series. There have been changes in the 10.7 cm solar radio flux monitoring program that have inevitably affected the data. These include the transition from manual to automatic processing, the ending of attempts to remove flare contamination from the data, programme upgrades, relocation, and consequent modification of the calibration process.

2.3.1. Flux Processing and Flare Contamination

From the beginning of the programme to the late 1970s, the flux values were processed by hand from paper charts. The antenna motions were automated using a mechanical system. Attempts were made to remove flare contamination from the measurements. The procedures were entirely empirical, and based on extensive experience acquired through many years of looking at the data. Moreover, the procedures only removed some of the flare contamination, with the effectiveness of the procedure varying with the character, intensity, and timing of the flare. In the late 1970s the level of staff support decreased and data processing became increasingly automated. Owing to the problems in developing a reliable means to consistently filter flare emissions from the data and also to meet the desire of some users to have the numbers as measured, flare filtering procedures were terminated in 1985.

2.3.2. Relocation and Calibration

In the early decades of the programme, the data were calibrated using blackbody cavities and by comparison with measurements made using a dual-horn calibration standard. This evolved into procedures using matched loads of known temperature and a measurement of signal level when the antenna was pointed at the zenith. That zenith temperature value included thermal emissions from the troposphere and those picked up from nearby trees and the ground. After some years of operation, the calibration horn was removed and put in storage.

In 1990 it became necessary to move the programme from its location in Algonquin Park, near Ottawa, to its current location at the Dominion Radio Astrophysical Observatory, near Penticton. Rather than repeat the process of calibrating the zenith temperature for the solar flux monitor antennas at the new, far drier environment, with fewer nearby trees, the calibration horn was recovered, restored, and fitted with new electronics, and the flux calibrations re-established against that standard. At the same time, the calibration procedure was changed to that described in Tapping (2013), which eliminated the need for zenith measurements and minimised errors due to ground radiation. Since then the data have been locked to periodic horn calibration checks. The move from Ottawa to Penticton, in addition to the programme upgrades and changes in the calibration process, may have resulted in a calibration difference. A value of about 2% has been suggested (see <http://www.leif.org/research/SHINE-2010-Microwave-Flux.pdf>).

2.3.3. Multiple Daily Flux Determinations

Originally, only one measurement was made each day, at local noon (1700 UT in Ottawa and then 2000 UT in Penticton). Then two additional daily flux determinations were added (three hours before and after local noon in summer; two hours before and after local noon in winter). There are long-term systematic differences between the three measurements that we have so far been unable to explain. These are most evident in winter. A combination of antenna pointing issues, low Sun, and hilly horizon are possible factors. In this study only the local noon measurements are used.

3. The Comparison Process

The indices used here are obtained and processed in a range of different ways, have diverse variational time-scales, and may suffer from various degrees of under-sampling. Before they can be usefully compared, they need to be rendered more statistically similar. Using daily whole-disc data, monthly averages are calculated, upon which are imposed a 10-month running mean. This provides additional smoothing while retaining more of the short-timescale information, at the expense of making adjacent data points less independent. Sunspot number and total sunspot area range from near zero to possibly thousands. The range (maximum value/minimum value) is very large. $F_{10.7}$ ranges from a quiet-Sun value of about 67 solar flux units to between three and four hundred solar flux units, although flare emissions can drive it far higher.

The sunspot number and total sunspot area data are used to produce proxies for $F_{10.7}$. These proxies are easier to compare with the indices and with each other because they are

more linearly related, are always non-zero, and have limited range. For the comparison we use the parameter

$$\beta(F_{10.7}, X) = \frac{O(F_{10.7}) - P(F_{10.7}, X)}{O(F_{10.7})}, \tag{1}$$

where $O(F_{10.7})$ is the observed value of $F_{10.7}$ and $P(F_{10.7}, X)$ is a proxy for $F_{10.7}$ derived using the index X , which in this case is either sunspot number or total sunspot area. This method of comparison has the advantage that the strong modulation of the data by the solar activity cycle is greatly reduced.

For the reasons given above, it is more convenient to compare total sunspot area with sunspot number, and the original and revised sunspot number by comparing their $F_{10.7}$ proxies:

$$\beta(A, X) = \frac{P(F_{10.7}, A) - P(F_{10.7}, X)}{P(F_{10.7}, X)}, \tag{2}$$

where A and X are $N_r, N_o, A_s, N_o,$ and $A_s, N_r,$ respectively.

4. The Proxies

Figure 2 shows the original (top) and the revised (bottom) sunspot number plotted against $F_{10.7}$. All the plotted data are monthly averages further smoothed with a 10-month running mean. To use sunspot number data to proxy the 10.7 cm solar radio flux, a totally empirical function of the form

$$P(F_{10.7}, N) = aN(2 - \exp(-bN)) + Q \tag{3}$$

works reasonably well. The quantities a and b are constants and Q is the quiet-Sun flux density, which is about 67 solar flux units. This equation fits the slight “knee” in the plot at a sunspot number of about 20, which is possibly due to the dominance of free-free thermal emission at low activity and the increased importance of thermal gyroresonance at higher levels of activity.

Using this model for the sunspot number-based proxies, we obtain the following equations for the $F_{10.7}$ proxies based on the observed and revised sunspot number data, respectively:

$$P(F_{10.7}, N_o) = 0.44N_o(2 - \exp(-0.031N_o)) + 67 \tag{4}$$

and

$$P(F_{10.7}, N_r) = 0.31N_r(2 - \exp(-0.019N_r)) + 67, \tag{5}$$

where the “o” and “r” subscripts refer to the “original” and “revised” sunspot number data. The constant 67 solar flux units is a hypothetical quiet-Sun value: the value corresponding to an absence of sunspots.

Similarly, Figure 3 shows $F_{10.7}$ plotted against smoothed values of total sunspot area, together with the fitted empirical function.

The fitted function relating $F_{10.7}$ and total sunspot area A_s is

$$P(F_{10.7}, A_s) = 0.5(2 - \exp(-0.001A_s))(-5 \times 10^{-9}A_s^2 + 0.067A_s) + 67. \tag{6}$$

This equation is used to generate a proxy for $F_{10.7}$ from the total sunspot area data.

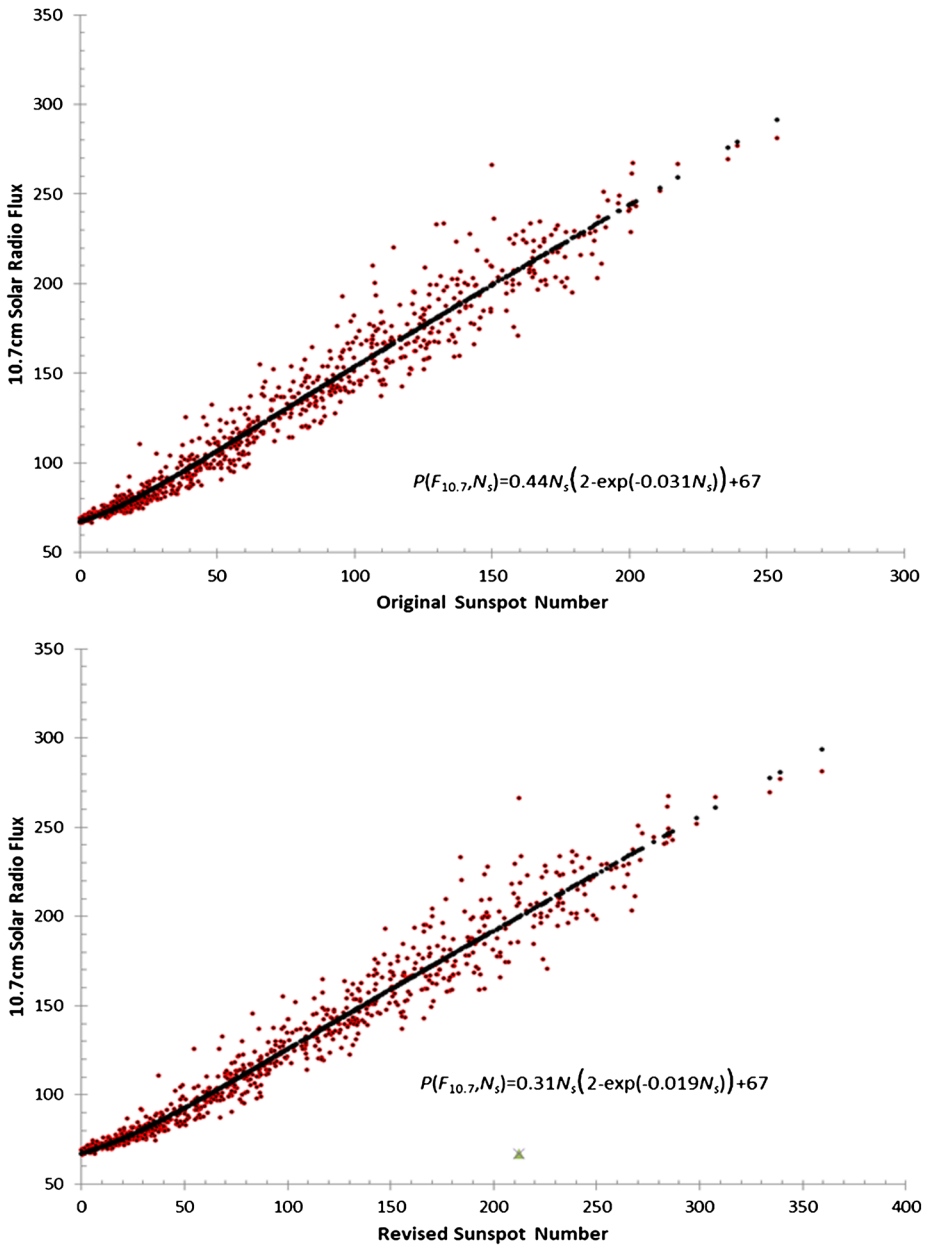


Figure 2 Plot of $F_{10.7}$ against original sunspot number (top) and revised sunspot number (bottom), together with fitted functions.

5. Comparisons

In all the comparison figures, unless specified otherwise, a scaled and offset plot of $F_{10.7}$ is included at the bottom of the plot, together with cycle numbers.

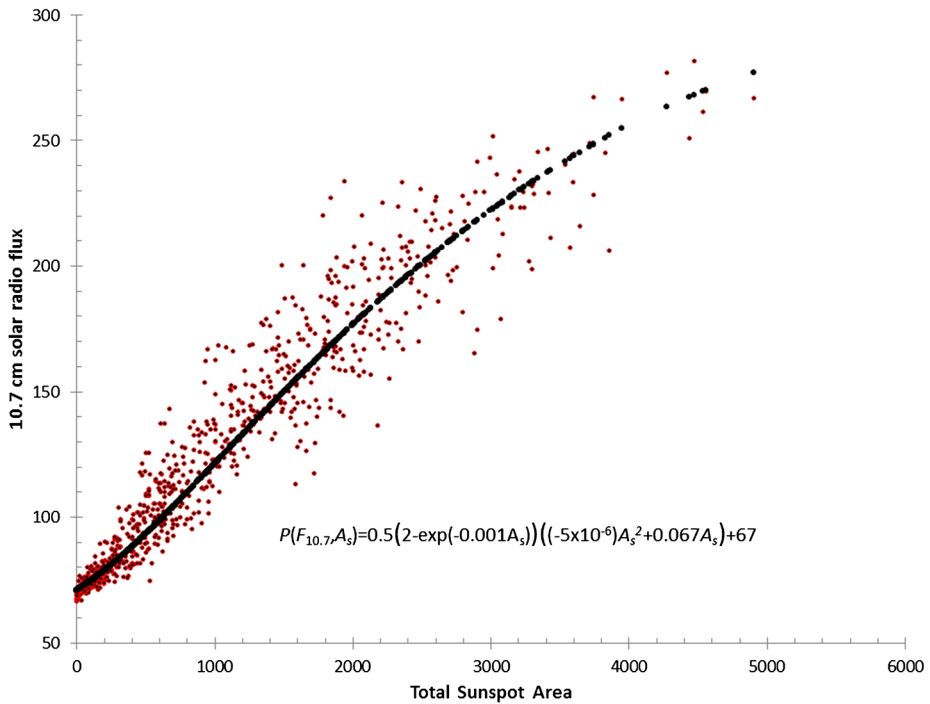


Figure 3 Smoothed $F_{10.7}$ values plotted against similarly smoothed values of the total sunspot area, together with the fitted function.

5.1. Original and Revised Sunspot Number

The plot in Figure 5 shows a comparison of the $F_{10.7}$ proxies derived from original and revised sunspot data. The scaling factor is taken out in the comparison process. Earlier than 1981, this is more or less the case. However, afterwards the revision involved extensive changes. It should be noted that the deviations discussed in by Tapping and Valdés (2011) began in 1981, which suggests that the deviation may be at least partially solar (see comparison of total sunspot area and the two sunspot number series in Figure 4).

5.2. $F_{10.7}$ and Sunspot Number

Deviations between $F_{10.7}$ and the proxies based on sunspot number since 1981 are evident for both the original and revised sunspot number data. This conclusion is unaffected by the revision. The spike at the beginning of the plots is almost certainly due to calibration and other issues in the early months of the $F_{10.7}$ record. The deviation in Cycle 24 was much reduced in the revised sunspot number plot. The plots differ significantly during the latter part of Cycle 24. In the comparison with the original sunspot number data there is a large excess of $F_{10.7}$. In the case of the revised data there is a spike corresponding with the resurgence of activity in the last half of the cycle, with the value of the excess declining again. The rising trend in $F_{10.7}$ compared with sunspot number is evident.

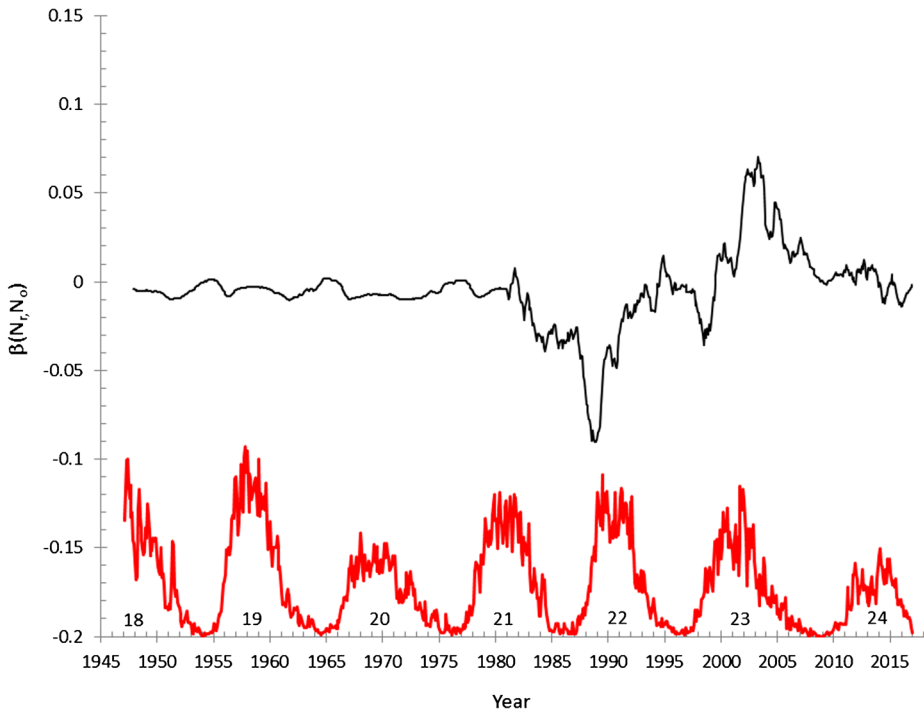


Figure 4 Comparison of original and revised sunspot number values since 1947 (black). At the bottom we show for reference a plot of $F_{10.7}$ and activity cycle numbers (red).

5.3. $F_{10.7}$ and Total Sunspot Area

As evident in Figure 1, $F_{10.7}$ is more highly correlated with sunspot number than it is with the total sunspot area index. Figure 6 shows the comparison of $F_{10.7}$ and total sunspot area. It would be difficult to conclude anything definite with this plot alone. However, the deviations in Cycles 21, 22, 23, and 24 visible in the sunspot number plots in Figures 5 and 6 are also present in the total sunspot area plot. The deviation in Cycle 24 strongly resembles that in the plot using the revised sunspot number data (Figure 6). However, Figure 7 also shows significant deviations around Cycle 19 that are not present in Figures 5 and 6. The differences in the plots indicate it would be useful to directly compare total sunspot area and sunspot number (using their $F_{10.7}$ proxies).

5.4. Total Sunspot Area and Sunspot Number

Comparison of the total sunspot area with total sunspot number gives an estimate of the area of the “mean sunspot”. The two comparisons of total sunspot area with sunspot number both show deviations in Cycles 21 and 23, indicating that sunspots are smaller in the rising part of the cycle and larger in the latter part. The deviations in Cycles 19 and 20 are smaller, and may indicate the reverse: larger spots in the rising part and smaller in the declining part. As in the case of the comparison of $F_{10.7}$ with the original sunspot number data, there is a spike in Cycle 24 that suggests a sunspot number deficit compared with the other indices. In addition, as in the comparison of $F_{10.7}$ with the revised sunspot number data, the deviation

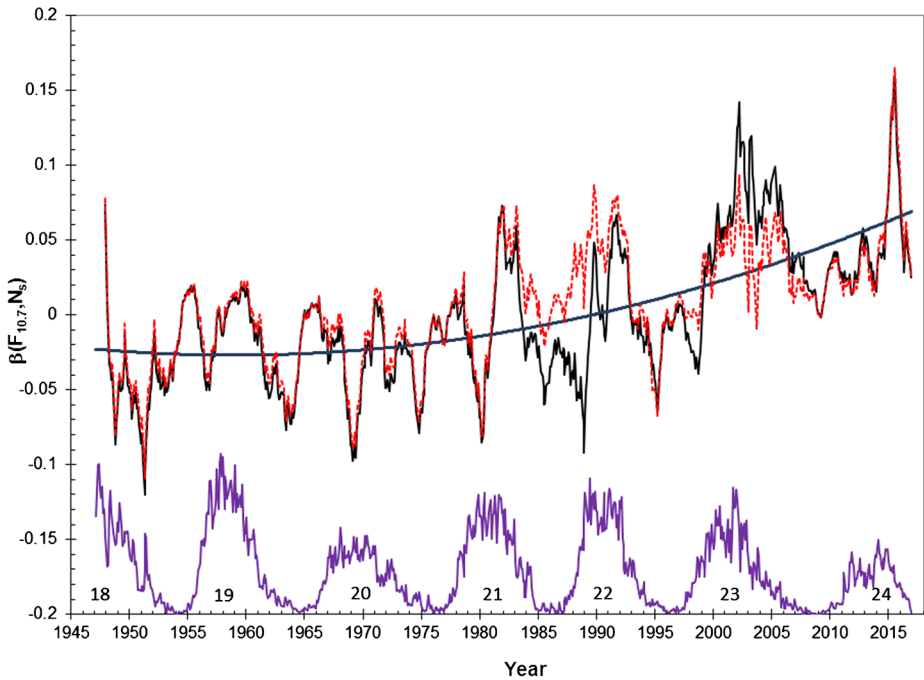


Figure 5 Comparison of $F_{10.7}$ with proxies based on original sunspot number (black solid line), and revised sunspot number (red dotted line). A second-order polynomial trend line has been added. At the bottom we show for reference a plot of $F_{10.7}$ and activity cycle numbers. The rise at the beginning of the record is due to the peak that is probably due to calibration issues.

in Cycle 24 is much smaller. The implication is that the revision of the sunspot number record has improved the data in that it brings the comparisons of $F_{10.7}$, total sunspot area, and revised sunspot number into agreement in Cycle 24.

6. Farther Back in Time

The total sunspot area record dates back to 1874, so the plot in Figure 8 can be taken back to that date. The patterns of deviation in Cycles 21 and 23 are possibly atypical. The only other event that stands out (slightly) in the record is Cycle 15, which shows a prolonged deficit in total sunspot area (smaller spots) around the maximum of the cycle. Most cycles show signs of smaller deficits. The lower plot is a scaled and offset record of revised sunspot number, together with the solar activity cycle numbers.

The 1981 changes are visible in comparisons between total sunspot area and the original and revised sunspot number. In Cycles 21 and 23, the occurrence of small spots in the early part of the cycle and larger spots later in the cycle is clear.

7. Discussion

All comparisons of the four activity indices, that is, original and revised sunspot number, total sunspot area, and 10.7 cm solar radio flux, show a significant change in solar behaviour

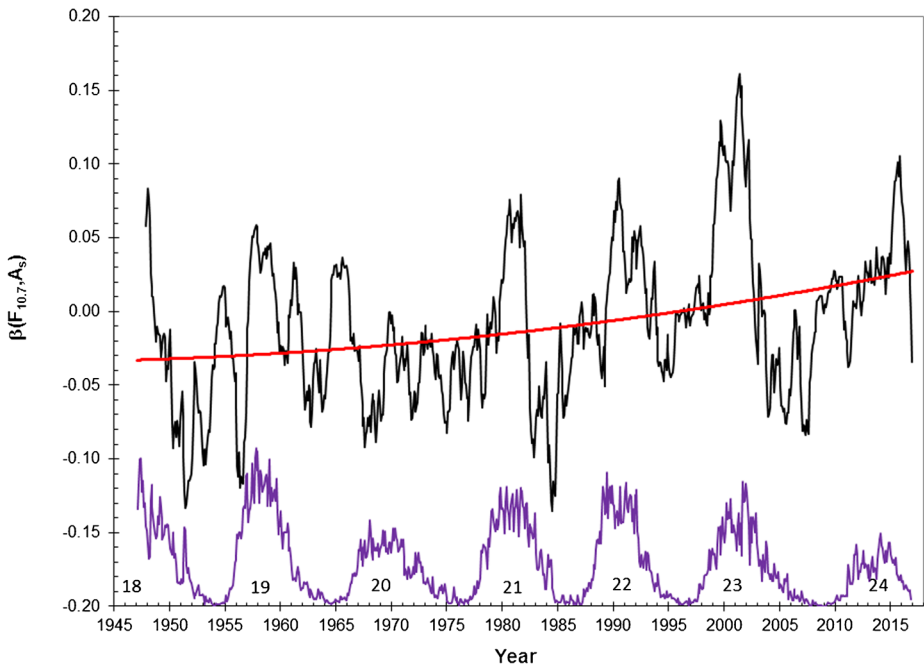


Figure 6 Comparison of $F_{10.7}$ with a proxy based on the total sunspot area index. A second-order trend line has been added.

in Cycle 21 and in some comparisons, growing short-term deviations in the maxima of subsequent cycles, culminating in Cycle 24. Unless there are issues with at least two of these indices, this probably marks a trend in changing solar behaviour.

These deviations show an excess of chromospheric/coronal activity as indicated by the $F_{10.7}$ index compared with photospheric activity as described by the sunspot number index, or conversely a deficit in photospheric activity compared with what would be expected on the basis of chromospheric/coronal activity. This latter statement is supported by a study by Livingston, Penn, and Svalgaard (2012), which reports a decline in sunspot number compared with $F_{10.7}$ beginning around 1995, which corresponds to the strong diversion in Cycle 23 as shown in Figure 5. Janardhan *et al.* (2015) studied in addition to $F_{10.7}$ and sunspot number the reduction in interplanetary scintillation (scintillation of distant radio sources due to turbulence and inhomogeneities in the solar wind). The continuing increase in $F_{10.7}$ compared with sunspot number suggests that since we are now in the declining phase of Cycle 24, this trend is likely to continue into Cycle 25.

It is possible that the excess of $F_{10.7}$ over observed sunspot number is related to the observed decline in sunspot umbral magnetic field strengths. The 10.7 cm solar radio flux comprises two main contributions: thermal free–free emission, and thermal gyroresonance. Their relative contribution depends largely on the strength of the ambient magnetic fields. The optical thickness of gyroresonance at the second or third harmonic of the electron gyrofrequency (f_g [GHz] = $2.8B$ [kilogauss]) is much higher than that for free–free emission, so where this condition is met, such as over sunspots, gyroresonance is likely to be the dominant emission component. However, Livingston, Penn, and Svalgaard (2012) pointed out that once the strength of a sunspot magnetic field falls below about 1500 Gauss, the contrast between it and the surrounding photosphere becomes very low. The magnetic field

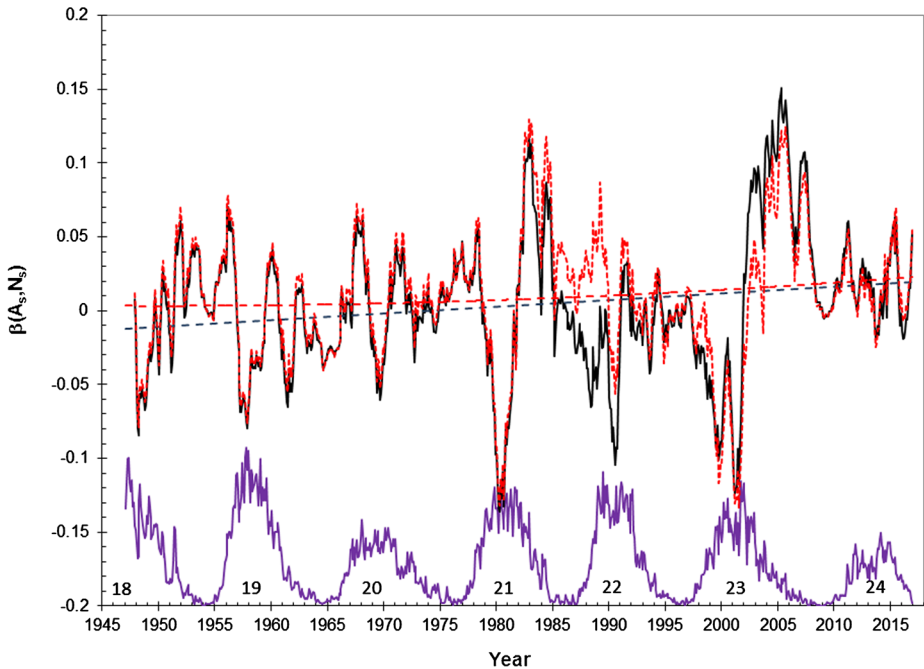


Figure 7 Comparison of the $F_{10.7}$ proxy based on total sunspot area with those based on original (black solid line) and revised (red dotted line) sunspot number.

strength in the corona overlying a sunspot will tend to be smaller than the umbral magnetic field strength due to spreading of the field, although this will be less above the centres of large spots. This could lead to sunspots being undercounted while still contributing to $F_{10.7}$. Similarly, the sunspot area data could be subject to the same issue.

It is premature to suggest that the Sun is in an immediate pre-Maunder or even pre-Dalton state, but an interesting aspect of the Maunder Minimum is that sunspot activity was low, but the activity cycles, as seen through secondary indicators like Be^{10} and C^{14} , continued at a low level, but higher than would have been expected on the basis of the sunspot number observations. This is clearly visible in the solar activity reconstructions described by Usoskin (2008).

Total sunspot area and sunspot number, both indicators of photospheric activity, are too highly related to be ideal parameters to be compared for sensitive detection of solar behavioural changes, but they are the only available direct indices of solar activity extending back in time beyond 1947. Total sunspot area measurements began in 1874; earlier than this, there is only the sunspot number. Comparison of total sunspot area and sunspot number back to 1874 shows that in addition to the deviations in Cycles 21 and 23, where sunspots were unusually small in the first half of the cycle and larger in the latter half, the only other distinct diversion was in Cycle 15, in 1920. There are several other smaller but possible candidates. There is some possible tendency in comparison for the larger diversions to occur in odd-numbered cycles. This is a tentative result only, but it does fit the 20–26 year solar magnetic activity cycle.

On the basis of the limited evidence here, Cycle 25, being an odd-numbered cycle, might show the deviations in mean sunspot size that occurred in Cycles 21 and 23. Comparisons with $F_{10.7}$ hint that there could be an even stronger deviation between coronal/chromospheric

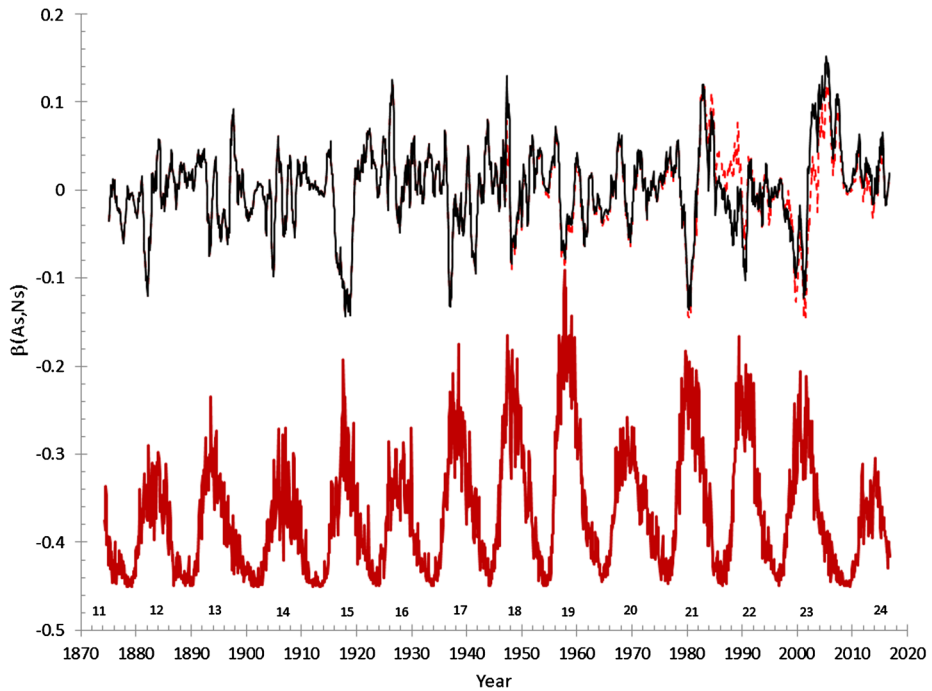


Figure 8 Comparison of total sunspot area and revised sunspot number values since 1874.

and photospheric activity in that cycle. Whether this will be an ongoing or another transient deviation is unclear.

Disclosure of Potential Conflicts of Interest The authors declare there are no conflicts of interest with respect to the contents of this paper or the data used in it.

Acknowledgements The authors owe a great vote of thanks to the Royal Observatory, Belgium, for the ongoing effort in providing the longest-duration, consistent direct record of solar activity available. Thanks are also due to the Royal Greenwich Observatory and now NASA for providing the also long-duration time-series of total sunspot area data. This research was supported by the National Research Council of Canada. One of the authors (CMM) was supported by the NRC Student Programme and by the University of Victoria, British Columbia.

References

- Athay, R.G., Warwick, C.S.: 1961, Indices of solar activity. *Adv. Geophys.* **8**, 1. [DOI](#). [ADS](#).
- Charbonneau, P., Blais-Laurier, G., St-Jean, C.: 2004, Intermittency and phase persistence in a Babcock–Leighton model of the solar cycle. *Astrophys. J. Lett.* **616**, L183. [DOI](#). [ADS](#).
- Charbonneau, P., St-Jean, C., Zacharias, P.: 2005, Fluctuations in Babcock–Leighton dynamo. I. Period doubling and transition to chaos. *Astrophys. J.* **619**, 613. [DOI](#). [ADS](#).
- Choudhuri, A.R.: 2003, In: Dwivedi, B.N., Parker, F.B.E.N. (eds.) *The Solar Dynamo as a Model of the Solar Cycle*, 103. [ADS](#).
- Clette, F., Lefèvre, L.: 2016, The new sunspot number: Assembling all corrections. *Solar Phys.* **291**, 2629. [DOI](#). [ADS](#).
- Clette, F., Lefèvre, L., Cagnotti, M., Cortesi, S., Bulling, A.: 2016, The revised Brussels–Locarno sunspot number (1981–2015). *Solar Phys.* **291**, 2733. [DOI](#). [ADS](#).

- Eddy, J.A.: 1976a, The Maunder minimum. *Science* **192**, 1189. DOI. ADS.
- Eddy, J.A.: 1976b, The sun since the Bronze Age. In: Williams, D.J. (ed.) *Physics of Solar Planetary Environments*, 958. ADS.
- Eddy, J.A.: 1977, Historical evidence for the existence of the solar cycle. In: White, O.R. (ed.) *The Solar Output and its Variation*, 51. ADS.
- Eddy, J.A.: 1979, Limits of historical evidence of solar variability. In: Robertson, P.C., Pepin, R.O., Eddy, J.A., Merrill, R.B. (eds.) *The Ancient Sun: Fossil Record in the Earth, Moon and Meteorites*, LPI Contributions **390**, 22. ADS.
- Janardhan, P., Bisoi, S.K., Gosain, S.: 2010, Solar polar fields during cycles 21 – 23: Correlation with meridional flows. *Solar Phys.* **267**, 267. DOI. ADS.
- Janardhan, P., Bisoi, S.K., Ananthakrishnan, S., Sridharan, R., Jose, L.: 2015, Solar and interplanetary signatures of a Maunder-like grand solar minimum around the corner – implications to near-Earth space. *Sun Geosph.* **10**, 147. ADS.
- Komitov, B., Kaftan, V.: 2004, The sunspot activity in the last two millenia on the basis of indirect and instrumental indexes: Time series models and their extrapolations for the 21st century. In: Stepanov, A.V., Benevolenskaya, E.E., Kosovichev, A.G. (eds.) *Multi-Wavelength Investigations of Solar Activity*, IAU Symposium **223**, 113. DOI. ADS.
- Krüger, A.: 1979, *Introduction to Solar Radio Astronomy and Radio Physics*. ADS.
- Kundu, M.R.: 1965, *Solar Radio Astronomy*. ADS.
- Livingston, W., Penn, M.J., Svalgaard, L.: 2012, Decreasing sunspot magnetic fields explain unique 10.7 cm radio flux. *Astrophys. J. Lett.* **757**, L8. DOI. ADS.
- Lockwood, M., Stamper, R.: 1999, Long-term drift of the coronal source magnetic flux and the total solar irradiance. *Geophys. Res. Lett.* **26**, 2461. DOI. ADS.
- Penn, M.J., Livingston, W.: 2006, Temporal changes in sunspot umbral magnetic fields and temperatures. *Astrophys. J. Lett.* **649**, L45. DOI. ADS.
- Penn, M.J., Livingston, W.: 2011, Long-term evolution of sunspot magnetic fields. In: Prasad Choudhary, D., Strassmeier, K.G. (eds.) *Physics of Sun and Star Spots*, IAU Symposium **273**, 126. DOI. ADS.
- Sarychev, A.P., Roshchina, E.M.: 2006, Total sunspot area as a solar activity index. *Solar Syst. Res.* **40**, 521. DOI. ADS.
- Tapping, K.F.: 2013, The 10.7 cm solar radio flux ($F_{10.7}$). *Space Weather* **11**, 394. DOI. ADS.
- Tapping, K.F., Valdés, J.J.: 2011, Did the sun change its behaviour during the decline of cycle 23 and into cycle 24? *Solar Phys.* **272**, 337. DOI. ADS.
- Usoskin, I.G.: 2008, A history of solar activity over millennia. *Living Rev. Solar Phys.* **5**, 3. DOI. ADS.